An isotope dilution model for partitioning of phenylalanine and tyrosine uptake by the liver of lactating dairy cows

Article

Accepted Version

It is advisable to refer to the publisher's version if you intend to cite from the work. See Guidance on citing.

To link to this article DOI: http://dx.doi.org/10.1016/j.jtbi.2017.12.016

Publisher: Elsevier

www.reading.ac.uk/centaur

CentAUR

Central Archive at the University of Reading

Reading's research outputs online

1   **An isotope dilution model for partitioning of phenylalanine and tyrosine uptake by the**

2   **liver of lactating dairy cows**

3

4   L.A. Crompton[a,*], L.L. McKnight[b], C.K. Reynolds[a], J.A.N. Mills[a], J.L. Ellis[b,c], M.D.

5   Hanigan[d], J. Dijkstra[c], B.J. Bequette[e,1] A. Bannink[c] and J. France[b]

6

7   [a] *Sustainable Agriculture and Food Systems Research Division, School of Agriculture, Policy*

8   *and Development, University of Reading, Whiteknights, Reading RG6 6AR, UK*

9   [b] *Centre for Nutrition Modelling, Department of Animal Biosciences, University of Guelph,*

10   *Ontario N1G 2W1, Canada*

11   [c] *Animal Nutrition Group, Wageningen University & Research, 6700 AH Wageningen, The*

12   *Netherlands*

13   [d] *Department of Dairy Science, Virginia Tech, 2080 Litton Reaves, Blacksburg, VA 24061,*

14   *USA*

15   [e] *Department of Animal & Avian Sciences, University of Maryland, College Park, MD 20742,*

16   *USA*

17

18   [1]Deceased

19

20   [*]**Corresponding author:** l.a.crompton@reading.ac.uk (L.A. Crompton)

21   **Abstract**

22   An isotope dilution model to describe the partitioning of phenylalanine (PHE) and tyrosine

23   (TYR) in the bovine liver was developed. The model comprises four intracellular and six

24   extracellular pools and various flows connecting these pools and external blood.

25   Conservation of mass principles were applied to generate the fundamental equations

26   describing the behaviour of the system in the steady state. The model was applied to datasets

27   from multi-catheterised dairy cattle during a constant infusion of [1-^{13}C] phenylalanine and

28   [2,3,5,6-^{2}H] tyrosine tracers. Model solutions described the extraction of PHE and TYR from

29   the liver via the portal vein and hepatic artery. In addition, the exchange of free PHE and

30   TYR between extracellular and intracellular pools was explained and the hydroxylation of

31   PHE to TYR was estimated. The model was effective in providing information about the

32   fates of PHE and TYR in the liver and could be used as part of a more complex system

33   describing amino acid metabolism in the whole animal.

34

37

2

1. Introduction

In ruminant production, the efficiency of milk protein synthesis from absorbed dietary nitrogen is quite low, 25-35 % (Hristov et al., 2004). In addition to the economic burden on the producer, urinary nitrogen losses contribute to greenhouse gas emissions and waterway contamination (Dijkstra et al., 2013). Milk protein synthesis is sensitive to essential amino acid supply, particularly phenylalanine (PHE). *In vivo* studies have demonstrated a reduction in milk protein concentrations when PHE is in low dietary supply (Rulquin and Pisulewski, 2000) and/or deficient in infusion mixtures (Doelman et al., 2015; Doepel et al., 2016). In the post-absorptive state, the liver has a key role in regulating PHE homeostasis. The liver can regulate the provision of PHE to peripheral tissues including the mammary gland, and remove PHE not used by the mammary gland or other peripheral tissues.

Net flux of PHE across the bovine liver has been examined *in vivo* using the arterio-venous difference technique (Tagari et al., 2004, 2008; Raggio et al., 2007; Berthiaume et al., 2006; Cantalapiedra-Hijar et al., 2014; Larsen et al., 2015). These studies reported a negative net flux of PHE, suggesting the liver is a major site of PHE utilization. In general, PHE has two metabolic fates, incorporation into protein or conversion to tyrosine (TYR) via PHE hydroxylase (oxidation). As a result, PHE catabolism always follows the pathway of TYR catabolism. Therefore, to examine PHE metabolism experimentally the simultaneous infusion of PHE and TYR stable isotope tracers is preferred. To resolve the kinetic data from such isotope infusion studies, mathematical models must be applied.

Mathematical models to describe PHE kinetics have varied in complexity (reviewed by Matthews, 2007). Simple models ignore the hydroxylation of PHE to TYR, whereas, more complex models aim to explain PHE conversion to TYR. In our previous publication (Crompton et al., 2014), we presented an eight pool compartmental model describing PHE and TYR metabolism in the mammary gland of lactating dairy cows. The present study is a

63   progression of this work and our previous model of leucine metabolism in the bovine liver

64   (France et al., 1998). The primary objective was to develop a steady state model of hepatic

65   PHE and TYR metabolism. The new model describes the partitioning of the PHE and TYR

66   between constitutive and export protein synthesis and potential other metabolic fates such as

67   hydroxylation of PHE to TYR.

68

69   **2. The model**

70   The scheme adopted is shown in Figure 1a. It contains four intracellular and six

71   extracellular pools. The intracellular pools are free PHE (pool 6), PHE in export protein

72   (pool 5), free TYR (pool 7) and TYR in export protein (pool 8), while the extracellular ones

73   represent portal vein PHE and TYR (pools 1 and 3), hepatic artery PHE and TYR (pools 2

74   and 4) and venous PHE and TYR (pools 9 and X). Pools external to the model and therefore

75   not specifically represented are indicated by the digit zero. The flows of PHE and TYR

76   between pools and into and out of the system are shown as arrowed lines.

77   The export protein-bound PHE pool has a single inflow: from free PHE, F_{56}, and two

78   efflows: secretion of export protein, F_{05}, and degradation, F_{65}. The intracellular free PHE

79   pool has four inflows: from the degradation of constitutive liver protein, F_{60}, from the

80   extracellular portal vein pool, F_{61}, from the hepatic artery pool, F_{62}, and from degradation of

81   export protein, F_{65}. The pool has four efflows: synthesis of constitutive liver protein, F_{06},

82   incorporation into export protein, F_{56}, hydroxylation to the intracellular free TYR pool, F_{76},

83   and outflow to the extracellular hepatic vein PHE pool, F_{96}. The intracellular free TYR pool

84   has five inflows: from the degradation of constitutive liver protein, F_{70}, from the extracellular

85   portal vein TYR pool, F_{73}, from the hepatic artery TYR pool, F_{74}, from the intracellular PHE

86   pool, F_{76}, and from the degradation of export protein, F_{78}. The pool has four efflows:

87   oxidation and TYR degradation products, $F_{07}^{(o)}$, synthesis of constitutive liver protein, $F_{07}^{(s)}$,

4

88   incorporation into export protein, F_{87}, and outflow to the extracellular hepatic vein TYR pool,

89   F_{X7}. The export protein-bound TYR pool has one inflow: from the intracellular free TYR

90   pool, F_{87}, and two efflows: secretion of export protein, F_{08}, and degradation, F_{78}.

91   The extracellular portal vein PHE pool has a single inflow: entry into the pool, F_{10}, and

92   two efflows: uptake by the liver, F_{61}, and bypass to the extracellular hepatic vein PHE pool,

93   F_{91}. The extracellular hepatic artery PHE pool has a single inflow: entry into the pool, F_{20},

94   and two efflows: uptake by the liver, F_{62}, and bypass to the extracellular hepatic vein PHE

95   pool, F_{92}. The same description applies to the corresponding TYR pools, i.e. pools 3 and 4

96   with flows F_{30}, F_{73}, F_{X3}, F_{40}, F_{74}, and F_{X4}, respectively. The extracellular hepatic vein PHE

97   pool has three inflows: bypass from the portal vein PHE pool, F_{91}, bypass from the hepatic

98   artery PHE pool, F_{92}, and release from the intracellular PHE pool, F_{96}, and one efflow from

99   the system, F_{09}. The same description applies to the corresponding TYR pool with flows F_{X3},

100   F_{X4}, F_{X7}, and F_{0X} respectively.

101   The schemes adopted for the movement of label are shown in Figures 1b and 1c.

102   Labelled [1-^{13}C]PHE and [2,3,5,6-^{2}H]TYR were infused into the jugular vein at a constant

103   rate for 8 h.. The enrichments of the extracellular pools are measured directly by taking

104   blood samples from the portal vein, hepatic artery and hepatic vein during the isotope

105   infusion. The enrichments of the intracellular pools can only be measured directly using

106   invasive procedures and to avoid such procedures, the enrichments of the intracellular pools

107   were set as a prescribed fraction of the corresponding arterial enrichment in this study. Blood

108   flow rate across the liver is measured by downstream dye dilution using *para*-amino hippuric

109   acid (PAH), but uncorrected for any N-acetylation that occurs across the liver (Katz and

110   Bergman, 1969). The scheme assumes that the only entry of label into the system is into the

111   PHE and TYR portal vein and hepatic artery pools via the effective infusion rates, flows I_1,

112   I_2, I_3, Φ_3, I_4, and Φ_4 and that the duration of the infusion is such that no label arises from the

113   breakdown of constitutive protein.

114   Conservation of mass principles can be applied to each pool in Figure 1a, b, c to generate

115   differential equations that describe the dynamic behaviour of the system. For total (isotopic

116   plus non-isotopic) PHE and TYR, these fundamental equations are (mathematical notation is

117   defined in Table 1):

118 $$\frac{dQ_1}{dt} = F_{10} - F_{61} - F_{91} \tag{1}$$

119 $$\frac{dQ_2}{dt} = F_{20} - F_{62} - F_{92} \tag{2}$$

120 $$\frac{dQ_3}{dt} = F_{30} - F_{73} - F_{X3} \tag{3}$$

121 $$\frac{dQ_4}{dt} = F_{40} - F_{74} - F_{X4} \tag{4}$$

122 $$\frac{dQ_5}{dt} = F_{56} - F_{05} - F_{65} \tag{5}$$

123 $$\frac{dQ_6}{dt} = F_{60} + F_{61} + F_{62} + F_{65} - F_{06} - F_{56} - F_{76} - F_{96} \tag{6}$$

124 $$\frac{dQ_7}{dt} = F_{70} + F_{73} + F_{74} + F_{76} + F_{78} - F_{07}^{(o)} - F_{07}^{(s)} - F_{87} - F_{X7} \tag{7}$$

125 $$\frac{dQ_8}{dt} = F_{87} - F_{08} - F_{78} \tag{8}$$

126 $$\frac{dQ_9}{dt} = F_{91} + F_{92} + F_{96} - F_{09} \tag{9}$$

127 $$\frac{dQ_X}{dt} = F_{X3} + F_{X4} + F_{X7} - F_{0X} \tag{10}$$

128   and for [^{13}C] labelled PHE and TYR:

129 $$\frac{dq_1}{dt} = I_1 - e_1\left(F_{61} + F_{91}\right) \tag{11}$$

130 $$\frac{\mathrm{d}q_2}{\mathrm{d}t} = I_2 - e_2\left(F_{62} + F_{92}\right) \tag{12}$$

131 $$\frac{\mathrm{d}q_3}{\mathrm{d}t} = I_3 - e_3\left(F_{73} + F_{X3}\right) \tag{13}$$

132 $$\frac{\mathrm{d}q_4}{\mathrm{d}t} = I_4 - e_4\left(F_{74} + F_{X4}\right) \tag{14}$$

133 $$\frac{\mathrm{d}q_5}{\mathrm{d}t} = e_6 F_{56} - e_5\left(F_{05} + F_{65}\right) \tag{15}$$

134 $$\frac{\mathrm{d}q_6}{\mathrm{d}t} = e_1 F_{61} + e_2 F_{62} + e_5 F_{65} - e_6\left(F_{06} + F_{56} + F_{76} + F_{96}\right) \tag{16}$$

135 $$\frac{\mathrm{d}q_7}{\mathrm{d}t} = e_3 F_{73} + e_4 F_{74} + e_6 F_{76} + e_8 F_{78} - e_7\left(F_{07}^{(o)} + F_{07}^{(s)} + F_{87} + F_{X7}\right) \tag{17}$$

136 $$\frac{\mathrm{d}q_8}{\mathrm{d}t} = e_7 F_{87} - e_8\left(F_{08} + F_{78}\right) \tag{18}$$

137 $$\frac{\mathrm{d}q_9}{\mathrm{d}t} = e_1 F_{91} + e_2 F_{92} + e_6 F_{96} - e_9 F_{09}$$

138   (19)

139 $$\frac{\mathrm{d}q_X}{\mathrm{d}t} = e_3 F_{X3} + e_4 F_{X4} + e_7 F_{X7} - e_X F_{0X} \tag{20}$$

140 and for [²H] labelled TYR:

141 $$\frac{\mathrm{d}\phi_3}{\mathrm{d}t} = \Phi_3 - \varepsilon_3\left(F_{73} + F_{X3}\right)$$

142   (21)

143 $$\frac{\mathrm{d}\phi_4}{\mathrm{d}t} = \Phi_4 - \varepsilon_4\left(F_{74} + F_{X4}\right) \tag{22}$$

144 $$\frac{\mathrm{d}\phi_7}{\mathrm{d}t} = \varepsilon_3 F_{73} + \varepsilon_4 F_{74} + \varepsilon_8 F_{78} - \varepsilon_7\left(F_{07}^{(o)} + F_{07}^{(s)} + F_{87} + F_{X7}\right) \tag{23}$$

145 $$\frac{\mathrm{d}\phi_8}{\mathrm{d}t} = \varepsilon_7 F_{87} - \varepsilon_8\left(F_{08} + F_{78}\right) \tag{24}$$

146 $$\frac{\mathrm{d}\phi_X}{\mathrm{d}t} = \varepsilon_3 F_{X3} + \varepsilon_4 F_{X4} + \varepsilon_7 F_{X7} - \varepsilon_X F_{0X} \tag{25}$$

147   When the system is in steady state with respect to both total and labelled PHE and TYR,

148   the derivative terms in equations (1)-(25) are zero. For the scheme assumed, the enrichment

149   of intracellular export protein-bound pools equalizes with that of the respective free pool in

150   steady state (i.e. $e_5 = e_6$, $e_8 = e_7$, $\varepsilon_8 = \varepsilon_7$) otherwise equations (5) and (15), and (8), (18) and

151   (24) are inconsistent. It should be noted that the liver is a heterogeneous mixture of cells, and

152   enrichment may differ at different parts of the organ where synthesis of export protein or

153   synthesis of constitutive protein takes place. Within cells there are different sites of synthesis

154   and oxidation, and differences in the sites of synthesis of individual proteins, with labelling of

155   the tracer amino acid highest at points near the cell surface and lowest at points near the sites

156   of degradation (see Waterlow, 2006). After equating intracellular enrichments and

157   eliminating redundant equations etc., equations (11) to (25) yield the following useful

158   identities:

159
$$I_1 - e_1\left(F_{61} + F_{91}\right) = 0 \tag{26}$$

160
$$I_2 - e_2\left(F_{62} + F_{92}\right) = 0 \tag{27}$$

161
$$e_1 F_{61} + e_2 F_{62} - e_6\left(F_{06} + F_{56} + F_{76} + F_{96} - F_{65}\right) = 0 \tag{28}$$

162
$$e_3 F_{73} + e_4 F_{74} + e_6 F_{76} - e_7\left(F_{07}^{(o)} + F_{07}^{(s)} + F_{87} + F_{X7} - F_{78}\right) = 0 \tag{29}$$

163
$$e_1 F_{91} + e_2 F_{92} + e_6 F_{96} - e_9 F_{09} = 0 \tag{30}$$

164
$$e_3 F_{X3} + e_4 F_{X4} + e_7 F_{X7} - e_X F_{0X} = 0 \tag{31}$$

165
$$\Phi_3 - \varepsilon_3\left(F_{73} + F_{X3}\right) = 0 \tag{32}$$

166
$$\Phi_4 - \varepsilon_4\left(F_{74} + F_{X4}\right) = 0 \tag{33}$$

167
$$\varepsilon_3 F_{73} + \varepsilon_4 F_{74} - \varepsilon_7\left(F_{07}^{(o)} + F_{07}^{(s)} + F_{87} + F_{X7} - F_{78}\right) = 0 \tag{34}$$

168
$$\varepsilon_3 F_{X3} + \varepsilon_4 F_{X4} + \varepsilon_7 F_{X7} - \varepsilon_X F_{0X} = 0 \tag{35}$$

169   To obtain steady state solutions to the model, it is assumed that PHE and TYR secreted

170   in export protein, CO_2 production and PHE and TYR removal from the hepatic vein pools

171   (i.e. F_{05}, F_{08}, $F_{07}^{(o)}$, F_{09} and F_{0X}, respectively) can all be measured experimentally. Further, it

172   is mathematically convenient to assume that percentage PHE extraction by the liver is the

173   same from the portal vein and hepatic artery supplies, giving:

174    $$\frac{F_{91}}{F_{92}}\left(=\frac{F_{61}}{F_{62}}\right)=\frac{F_{10}}{F_{20}} \tag{36}$$

175   Algebraic manipulation of equations (1)-(10) with the derivatives set to zero, together

176   with equations (26)-(36), gives the following unique solution:

177    $$F_{10}=I_1/e_1 \tag{37}$$

178    $$F_{20}=I_2/e_2 \tag{38}$$

179    $$F_{30}=\Phi_3/\varepsilon_3 \tag{39}$$

180    $$F_{40}=\Phi_4/\varepsilon_4 \tag{40}$$

181    $$\overline{F_{56}-F_{65}}=\widetilde{F}_{05} \tag{41}$$

182    $$\overline{F_{87}-F_{78}}=\widetilde{F}_{08} \tag{42}$$

183    $$F_{X7}=\frac{(e_4-e_3)(\varepsilon_X-\varepsilon_3)-(e_X-e_3)(\varepsilon_4-\varepsilon_3)}{(e_4-e_3)(\varepsilon_7-\varepsilon_3)-(e_7-e_3)(\varepsilon_4-\varepsilon_3)}\widetilde{F}_{0X} \tag{43}$$

184    $$F_{X4}=\frac{(\varepsilon_X-\varepsilon_3)\widetilde{F}_{0X}-(\varepsilon_7-\varepsilon_3)F_{X7}}{(\varepsilon_4-\varepsilon_3)} \tag{44}$$

185    $$F_{X3}=\widetilde{F}_{0X}-F_{X4}-F_{X7} \tag{45}$$

186    $$F_{73}=F_{30}-F_{X3} \tag{46}$$

187    $$F_{74}=F_{40}-F_{X4} \tag{47}$$

188    $$F_{07}^{(s)}=\frac{\varepsilon_3}{\varepsilon_7}F_{73}+\frac{\varepsilon_4}{\varepsilon_7}F_{74}-\widetilde{F}_{07}^{(o)}-\overline{F_{87}-F_{78}}-F_{X7} \tag{48}$$

9

189
$$F_{76} = \frac{e_7}{e_6}\left(\widetilde{F}_{07}^{(o)} + F_{07}^{(s)} + \overline{F_{87} - F_{78}} + F_{X7}\right) - \frac{e_3}{e_6}F_{73} - \frac{e_4}{e_6}F_{74} \tag{49}$$

190
$$F_{70} = \widetilde{F}_{07}^{(o)} + F_{07}^{(s)} + \overline{F_{87} - F_{78}} + F_{X7} - F_{73} - F_{74} - F_{76} \tag{50}$$

191
$$F_{91} = \frac{(e_9 - e_6)\widetilde{F}_{09}}{(e_1 - e_6) + (e_2 - e_6)\dfrac{F_{20}}{F_{10}}} \tag{51}$$

192
$$F_{92} = \frac{F_{20}}{F_{10}}F_{91} \tag{52}$$

193
$$F_{96} = \widetilde{F}_{09} - F_{91} - F_{92} \tag{53}$$

194
$$F_{61} = F_{10} - F_{91} \tag{54}$$

195
$$F_{62} = F_{20} - F_{92} \tag{55}$$

196
$$F_{06} = \frac{e_1}{e_6}F_{61} + \frac{e_2}{e_6}F_{62} - \overline{F_{56} - F_{65}} - F_{76} - F_{96} \tag{56}$$

197
$$F_{60} = F_{06} + \overline{F_{56} - F_{65}} + F_{76} + F_{96} - F_{61} - F_{62} \tag{57}$$

198   where for these equations the italics denote steady state values of flows and enrichments, the

199   tilde identifies a measured flow, and the over-lining (not to be confused with statistical mean)

200   indicates coupled flows (which cannot be separately estimated within the model). Equations

201   (37)-(57) were obtained through analytical solution (solving by hand) using conventional

202   linear algebra.

203

204   **3. Application**

205   Application of the model is illustrated using data from an experiment conducted in the

206   UK at the University of Reading with multi-catheterised mid-lactation Holstein-Friesian dairy

207   cows (average live-weight 667 kg). Animals were fed hourly by auto-feeders total mixed

208   ration (TMR) diets consisting of a 50:50 mixture on a dry matter basis of forage and

209   concentrate with the forage comprised of grass silage and chopped dried Lucerne in a 25:75

210 ratio on a dry matter basis. Concentrates were formulated to provide crude protein levels of

211 approximately 110 and 200 g per kg concentrate dry matter, such that average TMR crude

212 protein concentrations were 128 and 175 g/kg dry matter. Average daily dry matter intake

213 and milk yield for these animals were 22 kg/d and 30 L/d, respectively. The cows were given

214 constant abomasal infusions of water (18 L/d) for 4 d, followed by a buffered mixture of

215 essential amino acids for a further 6 d. The essential amino acids were administered at a

216 daily rate equivalent to the essential amino acids in 800 g milk protein. On the final day of

217 each abomasal infusion, animals received a primed, continuous infusion at a constant rate

218 into the jugular vein of $[1-^{13}C]$PHE (350 mg/h) and $[2,3,5,6-^2H]$TYR (100 mg/h) in sterile

219 saline for 8 h. Blood samples were taken simultaneously from catheters in the dorsal aorta

220 and the portal and hepatic veins at hourly intervals for the duration of the infusion for the

221 measurement of blood flow rate (by PAH dilution) and nutrient metabolism by the portal

222 drained viscera and liver. The final four blood samples taken 5-8 h after the infusion started

223 were averaged to provide steady state values.

224 The relevant experimental measurements are given in Table 2. They are reported for

225 three animals during the water infusion (2 low protein; 1 high protein diet) and one animal

226 during the amino acid infusion (high protein diet). Values are based on plasma rather than

227 whole blood. Phenylalanine and TYR measurements are based on free rather than total (i.e.

228 free plus bound) plasma PHE and TYR. The effective isotope infusion rates to the liver, I_1,

229 I_2, and I_3, Φ_3, I_4, Φ_4 were obtained from portal vein and arterial concentration and enrichment

230 of PHE and TYR and plasma flow rate in the portal vein and hepatic artery. The flows F_{09}

231 and F_{0X} were determined from hepatic vein PHE and TYR concentration and plasma flow

232 rate in the hepatic vein. The intracellular enrichments e_6, e_7 and ε_7 and the flows F_{05}, F_{08}

233 were not measured in the trial and had to be prescribed. Unpublished observations from our

234 laboratories demonstrated an intracellular to extracellular enrichment ratio of 0.3 for PHE and

235   TYR. Therefore, the missing intracellular free PHE and TYR enrichments, e_6, e_7, and ε_7 were

236   initially calculated as 0.3 times the corresponding arterial enrichments e_2, e_4, and ε_4

237   respectively. The export protein flows F_{05} and F_{08} were assigned values of 33.8 μmol/min

238   and 25.0 μmol/min respectively based on Raggio et al. (2007) and the relative proportion of

239   PHE and TYR in bovine serum albumin as a representative export protein (UniProt, 2017).

240   The flow $F_{07}^{(o)}$ was obtained from labelled CO_2 elevation in plasma flow across the liver and

241   hepatic vein PHE enrichment in sheep (Harris et al., 1992).

242   Calculated flows are presented in Table 3. Data provided were insufficient for

243   comprehensive statistical analysis; therefore the results must be interpreted with a degree of

244   caution. Initial solutions for each cow were non-physiological as some of the derived flows

245   gave negative values. Therefore, error bands of ±25% were placed around the values given

246   in Table 2 of the prescribed intracellular enrichments (e_6, e_7 and ε_7) and the measured

247   extracellular enrichments close to minimum detection levels (e_3, e_4 and e_X), and the solution

248   space mapped out by these bands was searched to find the best feasible solution for each cow.

249   The best feasible solution was obtained by sum of squares minimisation, where the sum of

250   squares to be minimised (SS) was defined as

251
$$SS = \left(1 - \frac{F_{60}}{F_{06}}\right)^2 + \left(1 - \frac{F_{70}}{F_{07}^{(s)}}\right)^2 + \left(\frac{F_{07}^{(s)}}{F_{06}} - \frac{F_{70}}{F_{60}}\right)^2$$

252   The assumptions underlying SS are constitutive liver protein synthesis and degradation are

253   moving towards equilibrium (as the cows were in mid-lactation), and the TYR to PHE ratio is

254   the same (or similar) in synthesised and degraded liver tissue. If no feasible solution could be

255   found, the error bands were expanded (up to ±40%) and the search repeated. The final

256   solutions are shown in Table 3.

257   An analysis of measurement errors in experimental enrichments and infusion rates on

258   model solutions was conducted. Mean values across all datasets were assigned to e_1, e_2, e_3,

259   e_4, e_6, e_7, e_9, e_x, ε_3, ε_4, ε_7, ε_x, I_1, I_2, Φ_3, Φ_4, F_{05}, $F_{07}^{(o)}$, F_{08}, F_{09}, F_{0X}. Inputs were then perturbed

260   in turn by 0, ±10% and ±20%. Each calculated flow (y, μmol/min) was then plotted against

261   the perturbation (x, %), and a five-point linear regression of y on x performed to determine

262   the slope of the line produced. The average slope was subsequently scaled by its

263   corresponding unperturbed average flow value, giving the scaled slopes dimensions of %

264   change in y per % change in x. Results of the error assessment are presented in Table 4. In

265   general, errors in infusion rates and measured flows had little impact on the sensitivity of

266   model solutions. However, errors in the measurement of isotopic enrichment and in assumed

267   intracellular enrichment values, cause marked changes in calculated flows, emphasising the

268   value of measuring intracellular enrichment directly.

269

270   **5. Discussion**

271   Improving nitrogen utilization in the ruminant, and consequently minimizing the

272   environmental impacts of ruminant production, is dependent on a clear understanding of post-

273   absorptive amino acid metabolism. The present model described the partitioning of the

274   indispensable amino acid, PHE (and TYR), in the bovine liver. The model gave estimates of

275   PHE flow across the liver, rates of PHE and TYR incorporation into constitutive and export

276   protein synthesis, and the rate of hydroxylation of PHE to TYR.

277   PHE and TYR enter the liver via the portal vein and hepatic artery. Amino acids

278   entering via the portal vein, the main blood supply to liver, represent recently absorbed or

279   released amino acids from the portal drained viscera and recirculating amino acids coming

280   from the mesenteric and hepatic arteries. Incoming amino acids via arterial blood reflect the

281   utilization of nutrients by peripheral tissues (Reynolds, 2006). The model predicted a greater

282   flow of PHE and TYR from the portal vein (90% of total inflow) than that from the hepatic

283 artery, which was expected as the portal vein accounted for the majority (84%) of liver blood

284 flow.

285 *In vivo* studies have observed a negative net flow of PHE across the bovine liver,

286 suggesting the liver is a major site of catabolism (Tagari et al., 2004, 2008; Reynolds, 2006;

287 Raggio et al., 2007; Berthiaume et al., 2006; Cantalapiedra-Hijar et al., 2014; Larsen et al.,

288 2015). In agreement, model solutions indicated a net negative flow of PHE and TYR across

289 the liver (efflow minus inflow, –396 and –298 µmol/min PHE and TYR respectively). Other

290 efflows of PHE and TYR from the liver included oxidation and incorporation into secreted

291 hepatic proteins. Oxidation rates varied greatly in individual animals (range 146 to 525

292 µmol/min), the highest value observed in the animal receiving the essential amino acid

293 infusion. The range of oxidation rates in animals receiving the control water infusion were

294 similar to those previously reported in lactating dairy cows (Raggio et al., 2007) fed low and

295 high protein diets. Oxidation rates used in the present model represent the sum of PHE and

296 TYR oxidation and combined PHE and TYR oxidation accounted for 23% of total PHE and

297 TYR inflow to the liver. However, the current model enables the conversion of PHE to TYR

298 to be estimated (F_{76}) which enables the combined oxidation to be separated. Phenylalanine

299 may either be used for protein synthesis or be converted to TYR which is catalysed by the

300 enzyme phenylalanine hydroxylase and is the first and rate limiting step in the metabolic

301 disposal of PHE. Tyrosine is then transaminated to *p*-hydroxyphenylpyruvate and ultimately

302 yields fumarate and acetoacetate, so that PHE and TYR give rise to both glucogenic and

303 ketogenic fragments. Tyrosine is not considered essential, because it can be synthesised from

304 PHE in addition to that provided from the diet. On average the model estimated that 23% of

305 inflow of PHE from blood (sum of hepatic artery and portal vein inflows) to the liver was

306 converted to TYR. Of the 178 µmol/min of PHE hydroxylated, 101 µmol/min were directly

307 oxidised and 77 µmol/min contributed 11% of the 717 µmol/min total TYR inflow (sum of

308   TYR from hepatic artery and portal vein and from PHE hydroxylation). Individual amino

309   acid oxidations as a percentage of liver inflow were estimated to be 13% for PHE and 29%

310   for TYR. Measuring TYR oxidation directly represents a challenge experimentally. In

311   general, deuterium labelled PHE is inadequate for quantifying PHE kinetics and oxidation,

312   which requires the use of carbon labelled PHE and by default, deuterium labelled TYR

313   (reviewed by Matthews, 2007).

314   Another efflow of PHE and TYR considered in the model was their incorporation into

315   hepatic export protein. The liver makes several export proteins of various functions.

316   Albumin is important for the maintenance of vascular osmotic pressure. Due to this critical

317   role, albumin synthesis is maintained across various mild physiological challenges, although

318   in more severe situations of nutrient shortage, albumin synthesis may decrease. Raggio et al.

319   (2007) determined export plasma protein synthesis rate in lactating dairy cows and assumed

320   that export plasma protein contained 5% PHE. The value thus obtained by Raggio et al.

321   (2007) was used in the present model to represent the flow of PHE into export protein (F_{05}).

322   Since plasma proteins are also derived from sources other than the liver, the assumption that

323   total plasma export protein synthesis is all hepatic in origin may well have overestimated the

324   flow of PHE into export protein to some degree in the current model. The incorporation of

325   TYR (F_{08}) into albumin was unknown and assumed equivalent to that of PHE after correcting

326   for the relative proportions of PHE and TYR in albumin. This assumption is recognized as a

327   limitation of the current modelling exercise. Specifically, the incorporation of individual

328   amino acids depends on the type of export protein; some export proteins may require

329   proportionally higher amounts of PHE or TYR. This limitation was circumvented in our

330   bovine mammary model (Crompton et al., 2014) as the export protein was milk and isotope

331   enrichment in milk was easily measured.

332   A unique feature of the present model is the description of intracellular PHE and TYR

333   partitioning. Constitutive hepatic protein degradation was the largest contributor to the free

334   PHE and TYR pools, followed by portal vein and hepatic artery delivery (PHE 72%, 22%,

335   6%; TYR 65%, 22%, 5%). It should be noted that these estimates are influenced by

336   assumptions which had to be made with respect to intracellular enrichments, as discussed

337   later. Flow of PHE and TYR into constitutive protein synthesis comprised 98% of total

338   synthetic flow. The ratio of PHE to TYR in synthesised constitutive protein and degraded

339   constitutive protein was the same in each animal (range 1.06 to 1.66) and averaged 1.30. The

340   ratio of constitutive protein synthesis to degradation was 1.1 for both PHE and TYR.

341   However, in mid to late lactation dairy cows, the ratio of PHE and TYR synthesis to

342   degradation should be equal. Model estimates of intracellular PHE and TYR partitioning

343   must be interpreted with caution due to methodological limitations and imposed assumptions.

344   For example, samples were taken from whole blood and free PHE and TYR concentrations

345   were quantified and considered in the model. Therefore the extent to which peptide bound

346   PHE and TYR contribute to constitutive protein synthesis and degradation flows cannot be

347   determined. As hepatic tissues were not sampled, isotopic enrichment of the intracellular

348   pools was estimated based on the sampled precursor pools. The choice of precursor pool

349   enrichment is central in the present model as with any measurement of protein synthetic rate

350   in the whole body or tissues (see Waterlow, 2006). The assumption that intracellular

351   enrichments were 0.30 of plasma was based on unpublished observations from an unrelated

352   in vivo trial from our laboratory. Using the same isotopes as the present study, average liver

353   homogenate free enrichment for PHE and TYR was 0.30 (SD 0.07; range 0.19-0.38) of

354   plasma enrichment in lactating dairy cattle. Initially, the model solved to give some non-

355   physiological flows and had to be re-solved by adjusting the intracellular enrichments and the

356   extracellular ones close to minimum detection levels using a least-squares minimisation

16

357   routine. Besides, the actual precursor pool for various constitutive and export proteins may

358   differ. The lack of homogeneity in activity at various parts of the liver indicates that

359   intracellular enrichment is not uniform throughout the liver, and enrichment in export protein

360   and constitutive protein therefore may differ. In particular, the precursor enrichment for

361   constitutive protein synthesis may be lower than that for export protein synthesis (Connell et

362   al., 1997). Due to lack of specific measurements, this observation could not be included in

363   the present model.

364   Another means of estimating intracellular enrichment would be to measure the

365   incorporation of label into proteins having a fast turnover rate in plasma. For example,

366   studies in humans use plasma VLDL apolipoprotein-B (Apo-B) enrichment as a hepatic

367   intracellular marker protein (Rafi et al., 2008). However, to our knowledge this approach has

368   not been undertaken in lactating dairy cattle and would likely yield the enrichment of the

369   precursor pool used for export protein synthesis, which is not necessarily the same as the

370   precursor pool for constitutive protein synthesis as discussed above.

371

372   **5. Conclusions**

373   The present 10-pool model allows for quantitative interpretation of the metabolism of PHE

374   and TYR in the liver of dairy cattle by showing their partition among different fates. The

375   model builds upon the existing eight pool model to describe protein turnover in the mammary

376   gland of the lactating dairy cow (Crompton et al., 2014). The exchange of PHE and TYR

377   between extracellular and intracellular pools was described and the hydroxylation of PHE to

378   TYR was estimated. In addition, the extraction of amino acids from the liver via the portal

379   vein and hepatic artery pools was represented. Upon application to dairy cattle during

380   infusion of $[1\text{-}^{13}C]$ phenylalanine and $[2,3,5,6\text{-}^{2}H]$ tyrosine tracers, the model was shown to

381   be effective in providing information about the fates of PHE and TYR in the liver, and could

382   be used as part of a more complex system describing amino acid metabolism in the whole

383   animal.

384   Just as accurate measurements of precursor pool enrichment are critical for the use of

385   labelled amino acids to determine tissue protein synthesis generally, the measurement of

386   intracellular free PHE and TYR enrichment are crucial components of the present model, yet

387   had to be estimated along with liver export protein in order to apply the model using the data

388   available from the experiment. If the model is to be applied more rigorously, future *in vivo*

389   studies should measure simultaneously the intracellular free PHE and TYR pools and liver

390   export protein, along with the plasma enrichments and flow rates measured in the present

391   work. Furthermore, the model could not be solved by algebraic means alone, as initially it

392   solved to give non-physiological flows and had to be re-solved by adjusting selected

393   enrichments using a least-squares minimisation routine. Therefore, the mathematical exercise

394   of cleaving the combined model and solving the PHE and TYR sub-models independently

395   but sequentially merits future investigation.

396

403 **References**

404 Berthiaume, R., Thivierge, M.C., Patton, R.A., Dubreuil, P., Stevenson, M., McBride, B.W.,

405   Lapierre, H., 2006. Effect of ruminally protected methionine on splanchnic metabolism of

406   amino acids in lactating dairy cows. J. Dairy Sci. 89, 1621-1634.

407 Cantalapiedra-Hijar, G., Lemosquet, S., Rodriguez-Lopez, J.M., Messad, F., Ortigues-Marty,

408   I., 2014. Diets rich in starch increase the posthepatic availability of amino acids in dairy

409   cows fed diets at low and normal protein levels. J. Dairy Sci. 97, 5151-5166.

410 Connell, A., Calder, A.G., Anderson, S.E., Lobley, G.E., 1997. Hepatic protein synthesis in

411   the sheep: effect of intake as monitored by use of stable-isotope-labelled glycine, leucine

412   and phenylalanine. Br. J. Nutr. 77,255-271.

413 Crompton, L.A., France, J., Reynolds, C.K., Mills, J.A.N., Hanigan, M.D., Ellis, J.L.,

414   Bannink, A., Bequette, B.J., Dijkstra, J., 2014. An isotope dilution model for partitioning

415   phenylalanine and tyrosine uptake by the mammary gland of lactating dairy cows. J.

416   Theor. Biol. 359, 54-60.

417 Dijkstra, J., Oenema, O., Van Groenigen, J.W., Spek, J.W., van Vuuren, A.M., Bannink, A.,

418   2013. Diet effects on urine composition of cattle and N_2O emissions. Animal 7 (suppl. 2),

419   292-302.

420   Doelman, J., Curtis, R.V., Carson, M., Kim, J.J.M., Metcalf, J.A., Cant, J.P., 2015. Essential

421   amino acid infusions stimulate mammary expression of eukaryotic initiation factor 2Bε but

422   milk protein yield is not increased during an imbalance. J. Dairy Sci. 98:4499-4508.

423   Doepel, L., Hewage, I.I., Lapierre, H., 2016. Milk protein yield and mammary metabolism

424   are affected by phenylalanine deficiency but not by threonine or tryptophan deficiency. J.

425   Dairy Sci. 99, 3144-3156.

426   France, J., Hanigan, M.D., Reynolds C.K., Dijkstra J., Crompton, L.A., Maas J.A., Bequette,

427   B.J., Metcalf J.A., Lobley, G.E., MacRae, J.C., Beever, D.E., 1998. An isotope dilution

428   model for partitioning leucine uptake by the bovine liver. J. Theor. Biol. 198, 121-133.

429   Harris, P.A., Skene, P.A., Buchan, V., Milne, E., Calder, A.G., Anderson, S.E., Connell, A,

430   Lobley, G.E., 1992. Effect of food intake on hind-limb and whole-body protein

431   metabolism in young growing sheep: chronic studies based on arterio-venous techniques.

432   Br. J. Nutr. 68, 389-407.

433   Hristov, A.N., Price, W.J., Shafii, B., 2004. A meta-analysis examining the relationship

434   among dietary factors, dry matter intake, and milk and milk protein yield in dairy cows. J.

435   Dairy Sci. 87, 2184-2196.

436   Katz, M.L., Bergman, E.N., 1969. Simultaneous measurements of hepatic and portal venous

437   blood flow in the sheep and dog. Am. J. Physiol. 216, 946-952.

438   Larsen, M., Galindo, C., Ouellet, D.R., Maxin, G., Kristensen, N.B., Lapierre, H., 2015.

439   Abomasal amino acid infusion in postpartum dairy cows: Effect on whole-body,

440   splanchnic, and mammary amino acid metabolism. J. Dairy Sci. 98, 7944-7961.

441   Matthews, D.E., 2007. An overview of phenylalanine and tyrosine kinetics in humans. J.

442   Nutr. 137, 1549S-1555S.

443   Rafii, M., McKenzie, J.M., Roberts, S.A., Steiner, G., Ball, R.O., Pencharz, P.B., 2008. *In*

444   *vivo* regulation of phenylalanine hydroxylation to tyrosine, studied using enrichment in

445 apoB-100 In vivo regulation of phenylalanine hydroxylation to tyrosine, studied using

446 enrichment in apoB-100. Am J Physiol Endocrinol Metab, 294(2), E475-E479.

447 Raggio, G., Lobley, G.E., Berthiaume, R., Pellerin, D., Allard, G., Dubreuil, P., Lapierre, H.,

448 2007. Effect of protein supply on hepatic synthesis of plasma and constitutive proteins in

449 lactating dairy cows. J. Dairy Sci. 90, 352-359.

450 Reynolds, C.K., 2006. Splanchnic metabolism of amino acids in ruminants, in: Sejrsen, K.,

451 Hvelplund, T., Nielsen, M.O., (Eds), Ruminant Physiology: Digestion, metabolism and

452 impact of nutrition on gene expression, immunology and stress. Wageningen Academic

453 Press, Wageningen, the Netherlands, pp. 225-248.

454 Rulquin, H., Pisulewski, P., 2000. Effects of duodenal infusions of graded amounts of Phe on

455 mammary uptake and metabolism in dairy cows. J. Dairy Sci. 83(Suppl. 1), 267-268.

456 Tagari, H., Webb Jr., K., Theurer, B., Huber, T., DeYoung, D., Cuneo, P., Santos, J.E.P.,

457 Simas, J., Sadik, M., Alio, A., Lozano, O., Delgado-Elorduy, A., Nussio, L., Nussio, C.,

458 Santos, F., 2004. Portal drained visceral flux, hepatic metabolism, and mammary uptake of

459 free and peptide-bound amino acids and milk amino acid output in dairy cows fed diets

460 containing corn grain steam flaked at 360 or steam rolled at 490 g/L. J. Dairy Sci. 87, 413-

461 430.

462 Tagari, H., Webb Jr., K., Theurer, B., Huber, T., DeYoung, D., Cuneo, P., Santos, J.E.P.,

463 Simas, J., Sadik, M., Alio, A., Lozano, O., Delgado-Elorduy, A., Nussio, L., Bittar,

464 C.M.M., Santos, F., 2008. Mammary uptake, portal-drained visceral flux, and hepatic

465 metabolism of free and peptide-bound amino acids in cows fed steam-flaked or dry-rolled

466 sorghum grain diets. J. Dairy Sci. 91, 679-697.

467 UniProt Consortium, 2017. UniProt: the universal protein knowledgebase. Nucleic Acids

468 Res. 45, D158-D169.

469 Waterlow, J.C. 2006. Protein turnover. CAB International, Wallingford, UK.

470

471   **Table 1.** Principle symbols used for the kinetic model.

F_{ij}	Flow of PHE[a] or TYR[a] to pool i from j; F_{i0} denotes an external flow into pool i and F_{0j} denotes a flow from pool j out of the system	μmol/min
I_i	Effective rate of constant infusion of ^{13}C labelled PHE or TYR into primary pool i	μmol/min
Φ_i	Effective rate of constant infusion of ^{2}H labelled TYR into primary pool i	μmol/min
Q_i	Quantity of PHE[a] or TYR[a] in pool i	μmol
q_i	Quantity of ^{13}C labelled PHE or TYR in pool i	μmol
ϕ_i	Quantity of ^{2}H labelled TYR in pool i	μmol
e_i	Enrichment of ^{13}C PHE or TYR in pool i: ($= q_i/Q_i$)	atoms % excess/μmol
ε_i	Enrichment of ^{2}H TYR in pool i: ($=\phi_i/Q_i$)	atoms % excess/μmol
t	Time	min

472
473   [a]Total material (*i.e.* tracee + tracer).
474

Table 2. Experimental and other inputs.

Cow		323/14	341/29	6031/42	6132/43[a]
Dietary CP (g/kg)		175	128	128	175
Milk yield (kg/d)		25.8	24.1	24.2	25.3
Plateau	e_1	2.19	3.37	2.79	2.10
enrichment (APE)	e_2	3.58	5.51	4.31	3.32
	$e_3{}^{b}$	0.15	0.18	0.18	0.32
	$e_4{}^{b}$	0.28	0.30	0.30	0.43
	$e_6{}^{b}$	1.07	1.65	1.29	1.00
	$e_7{}^{b}$	0.08	0.09	0.09	0.13
	e_9	2.14	3.54	2.70	2.00
	$e_X{}^{b}$	0.25	0.32	0.28	0.39
	ε_3	0.76	1.16	0.85	0.79
	ε_4	1.12	1.97	1.21	1.15
	$\varepsilon_7{}^{b}$	0.34	0.59	0.36	0.35
	ε_X	0.73	1.23	0.83	0.74
Flow (μmol/min)	I_1	52.6	44.5	53.7	56.9
	I_2	24.2	36.6	16.5	9.55
	Φ_3	19.0	12.2	16.5	16.3
	Φ_4	8.49	10.4	4.99	2.72
	F_{05}	33.8	33.8	33.8	33.8
	$F_{07}^{(o)}$	211	146	351	525
	F_{08}	25.0	25.0	25.0	25.0
	F_{09}	2595	1777	1938	2473
	F_{0X}	2858	1399	2034	2012

477
478 [a]Essential amino acid infusion
479 [b]Initial value
480
481

23

Table 3. Phenylalanine and tyrosine uptake and partition by the liver for four lactating dairy cows obtained using the ten-pool model (symbols are defined in the text and Table 1).

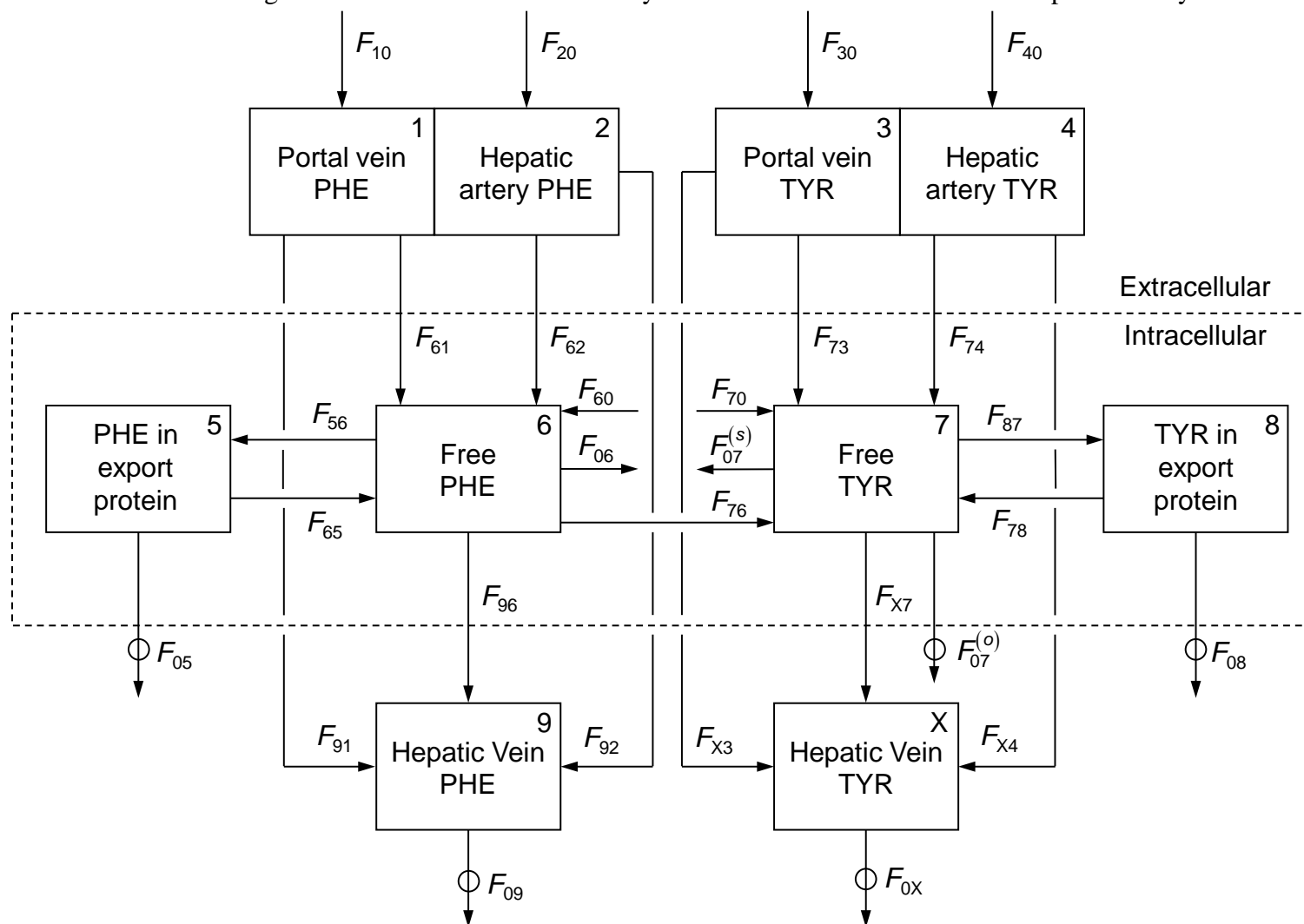| Cow		323/14	341/29	6031/42	6132/43
Flow (µmol/min)	F_{10}	2403	1319	1921	2711
	F_{20}	676	665	382	288
	F_{30}	2486	1048	1951	2072
	F_{40}	756	530	414	237
	$\overline{F_{56} - F_{65}}$	33.8	33.8	33.8	33.8
	$\overline{F_{87} - F_{78}}$	25.0	25.0	25.0	25.0
	F_{X7}	547	308	215	300
	F_{X4}	534	412	287	187
	F_{X3}	1778	679	1532	1525
	F_{73}	708	369	419	547
	F_{74}	223	118	127	50
	$F_{07}^{(s)}$	2323	1225	1713	1476
	F_{76}	138	70	172	332
	F_{70}	2037	1147	1586	1397
	F_{91}	1597	967	1366	1935
	F_{92}	449	487	272	205
	F_{96}	548	323	300	333
	F_{61}	806	353	555	776
	F_{62}	227	178	110	82
	F_{06}	2455	1568	2071	2444
	F_{60}	2143	1465	1911	2284
Adjusted	$e_3{}^{[a]}$	0.19	0.19	0.16	0.25
plateau	$e_4{}^{[a]}$	0.32	0.38	0.35	0.54
enrichment (APE)	$e_6{}^{[a]}$	0.81	1.09	0.79	0.61
	$e_7{}^{[a]}$	0.10	0.11	0.11	0.16
	$e_X{}^{[a]}$	0.20	0.23	0.18	0.26
	$\varepsilon_7{}^{[a]}$	0.25	0.39	0.22	0.21

[a]Final value

Table 4. Average slope (%) for each of the flows calculated by the model obtained by perturbing each input in turn[a].

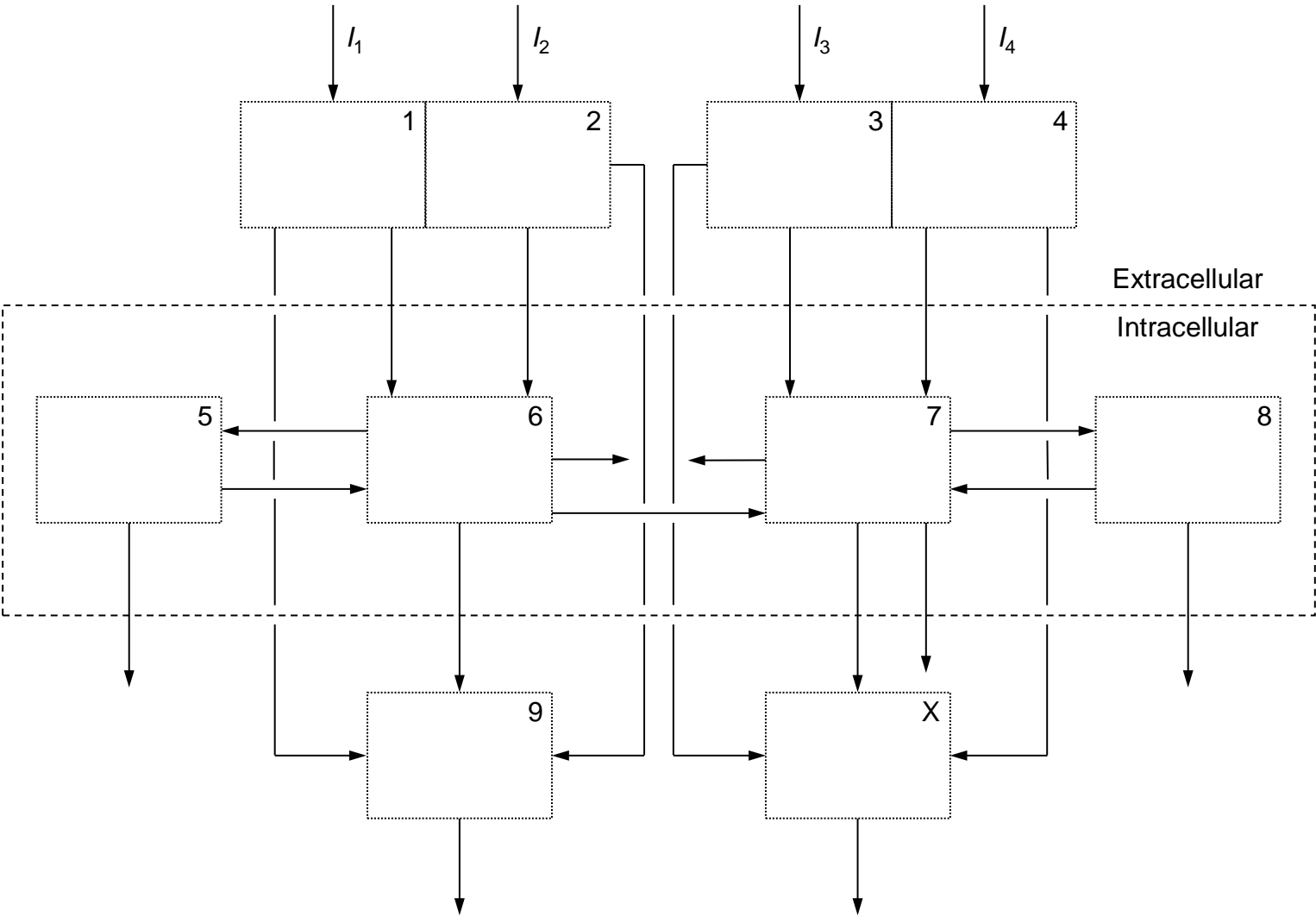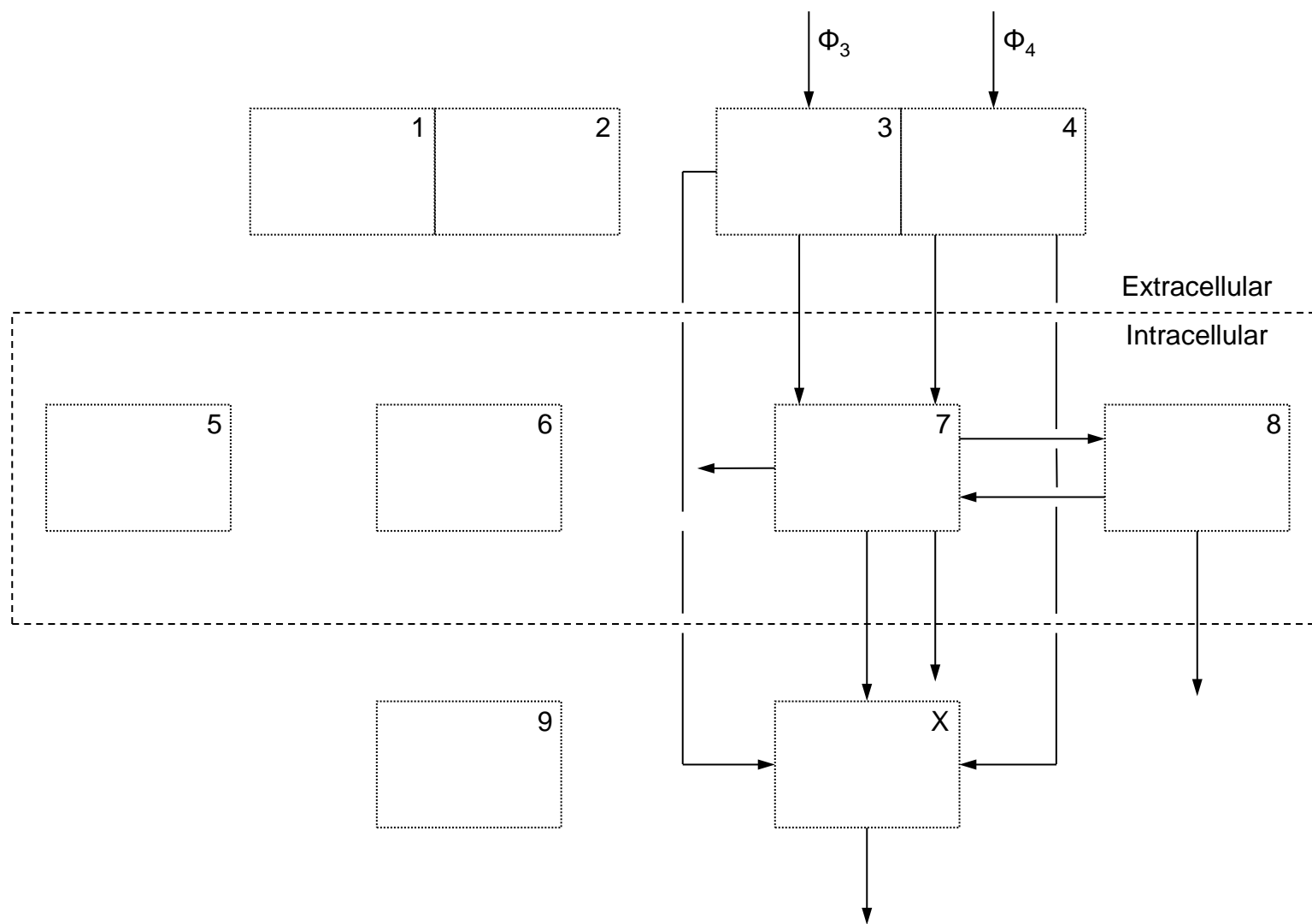| Flow	Unperturbed (μmol/min)[b]	Input perturbed[c]																				
		e_1	e_2	e_3	e_4	e_6	e_7	e_9	e_X	ε_3	ε_4	ε_7	ε_X	I_1	I_2	Φ_3	Φ_4	F_{05}	$F_{07}^{(o)}$	F_{08}	F_{09}	F_{0X}
F_{10}	2086													1.0								
F_{20}	547														1.0							
F_{30}	1862															1.0						
F_{40}	519																1.0					
$\overline{F_{56}-F_{65}}$	34																			1.0		
$\overline{F_{87}-F_{78}}$	25																				1.0	
F_{X7}	260			-7.6	-3.4		-0.64		9.2	16	3.8	0.62	-16									1.0
F_{X4}	309			-8.5	-3.8		-0.71		10	5.2	1.2	0.20	-5.2									1.0
F_{X3}	1522			3.0	1.4		0.25		-3.7	-3.8	-0.91	-0.15	3.8									1.0
F_{73}	341			-13	-6.1		-1.1		16	17	4.1	0.65	-17			5.5						-4.5
F_{74}	210			12	5.6		1.0		-15	-7.7	-1.8	-0.29	7.6				2.5					-1.5
$F_{07}^{(s)}$	1626							0.18		3.8	1.6	-1.2	-4.2			3.8	1.6	-0.18		-0.02		-4.2
F_{76}	136			-3.3	-1.9	-1.0	2.1		4.1	6.6	2.8	-2.1	-7.4			3.3	1.0					-3.3
F_{70}	1512			0.30	0.17	0.09	-0.19		-0.37	3.5	1.5	-1.1	-3.9			2.6	1.3					-2.9
F_{91}	1488	-1.0	-0.41			-0.08		1.5						0.33	-0.33						1.0	
F_{92}	391	-1.0	-0.41			-0.08		1.5						-0.68	0.67						1.0	
F_{96}	366	5.2	2.1			0.39		-7.5						-0.64	0.63						1.0	
F_{61}	598	2.5	1.0			0.19		-3.6						2.7	0.82							-2.5
F_{62}	157	2.5	1.0			0.19		-3.6						1.7	1.8							-2.5
F_{06}	2163	3.1	1.3	0.21	0.12	-1.1	-0.13	-3.3	-0.26	-0.42	-0.18	0.14	0.46	3.1	1.3	-0.21	-0.06	-0.02			-3.3	0.21
F_{60}	1944	3.4	1.4			-1.2		-3.6						2.3	1.2							-2.5

[a] The slope for each flow is expressed relative to the value of the flow obtained when no perturbation is made. Only slopes which differ from zero are shown.
[b] Values calculated from the mean of inputs reported in Table 2.
[c] Model solved by perturbing each input in turn by 0%, ±10% and ±20%.

494 **Figure 1**. Scheme for the uptake and utilisation of PHE and TYR by the liver of lactating dairy cows: (a) total PHE and TYR, (b) [^{13}C] labelled
495 PHE and TYR and (c) [^{2}H] labelled TYR. Nomenclature is defined in Table 1. Represented pools are numbered 1 to X and labelled in Figure
496 1a. The small circles in Figure 1a indicate flows out of the system which need to be measured experimentally.

497 (a)

498

I_1 I_2 I_3 I_4

| 1 | 2 | | 3 | 4 |

Extracellular

Intracellular

| 5 | 6 | | 7 | 8 |

| 9 | | X |

499   (b)

Φ_3　Φ_4

	1		2

	3		4

Extracellular

Intracellular

| | 5 | | | 6 | | | 7 | | | 8 |

| | 9 | | | X |

500　(c)

28